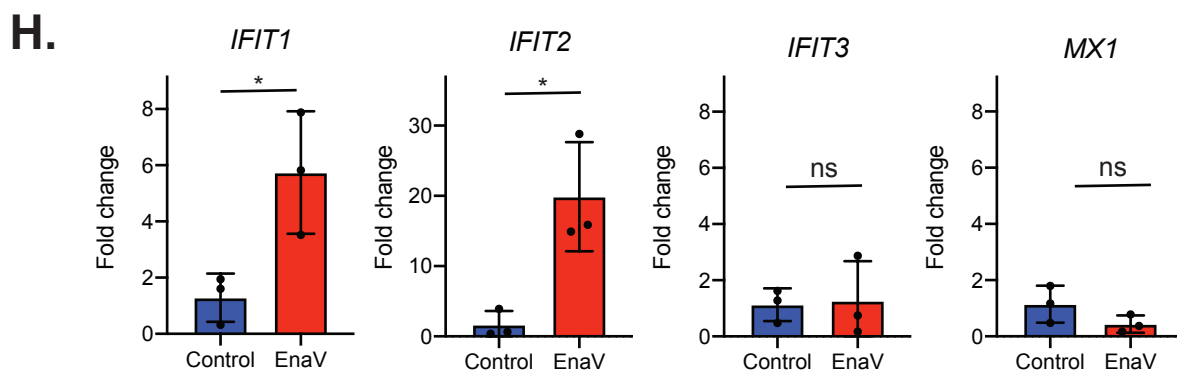
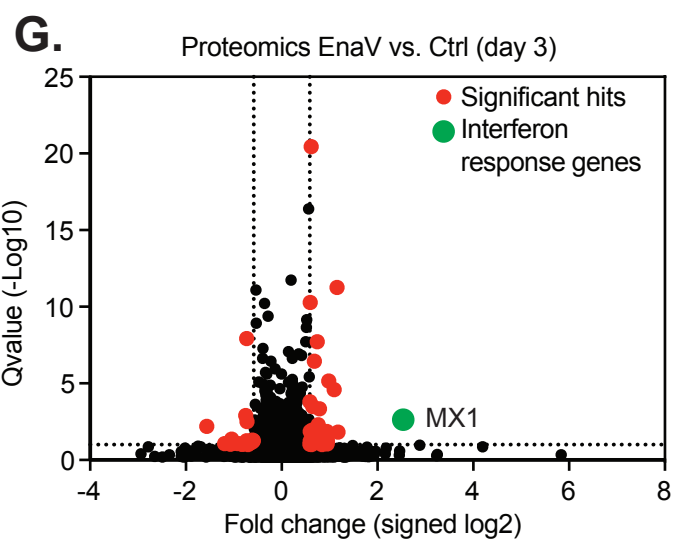
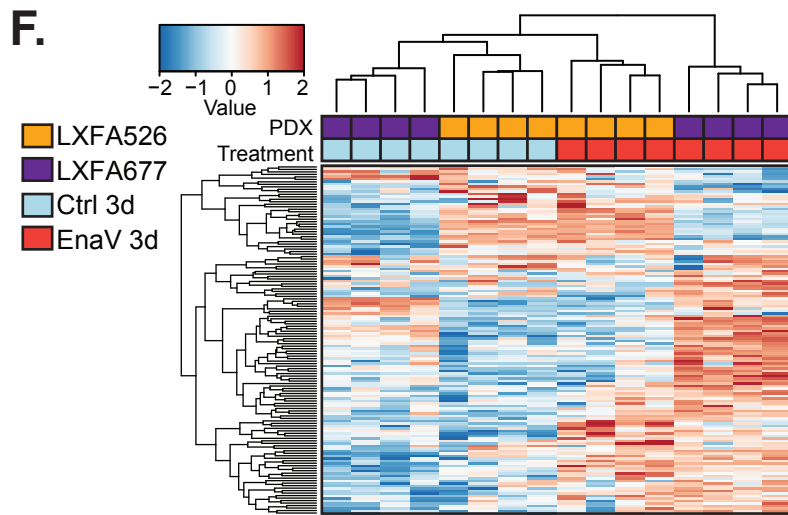
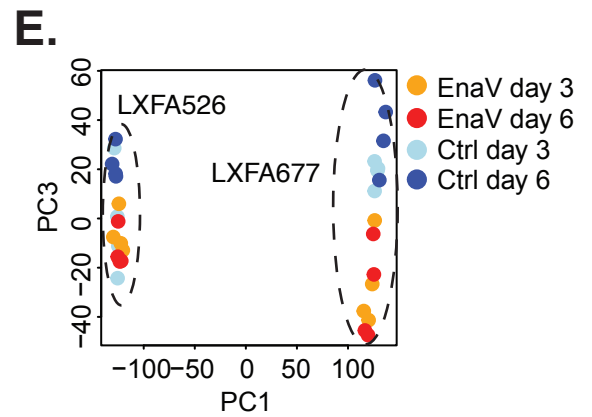
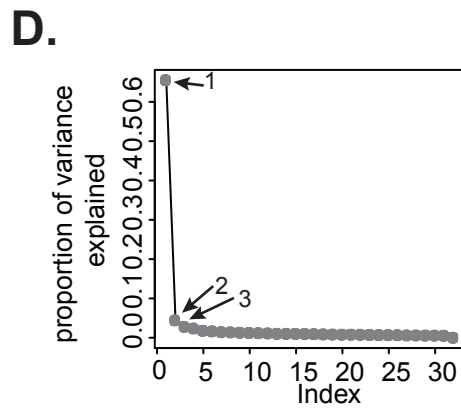
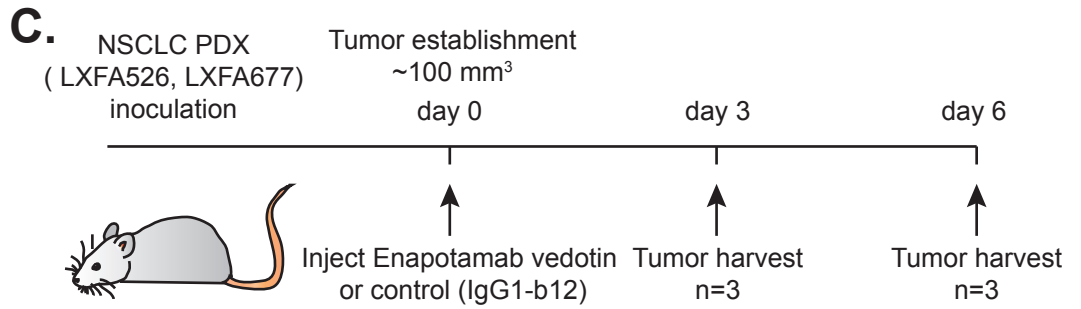
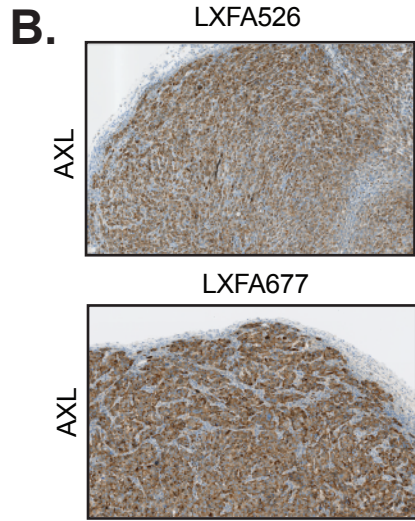
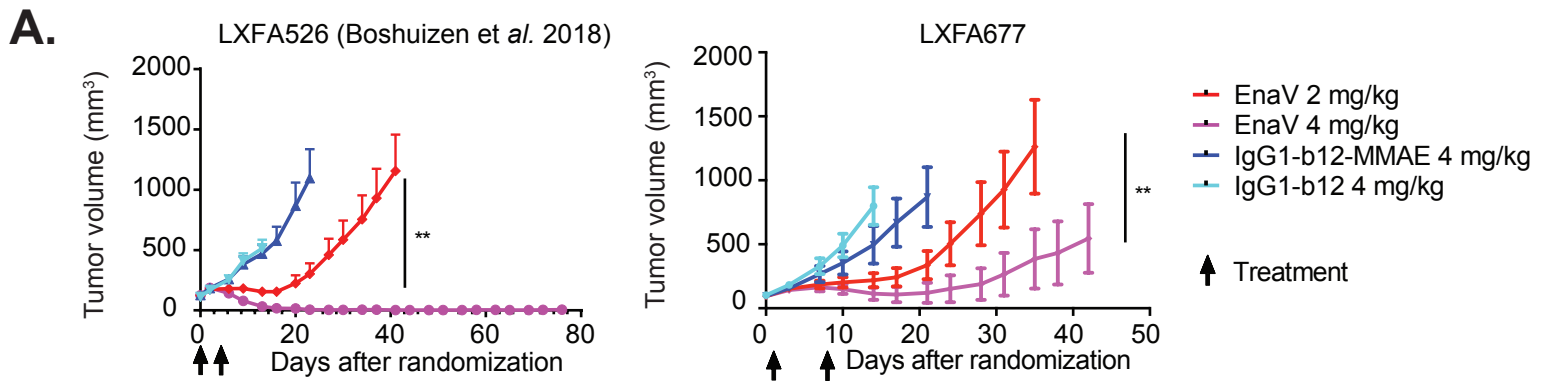


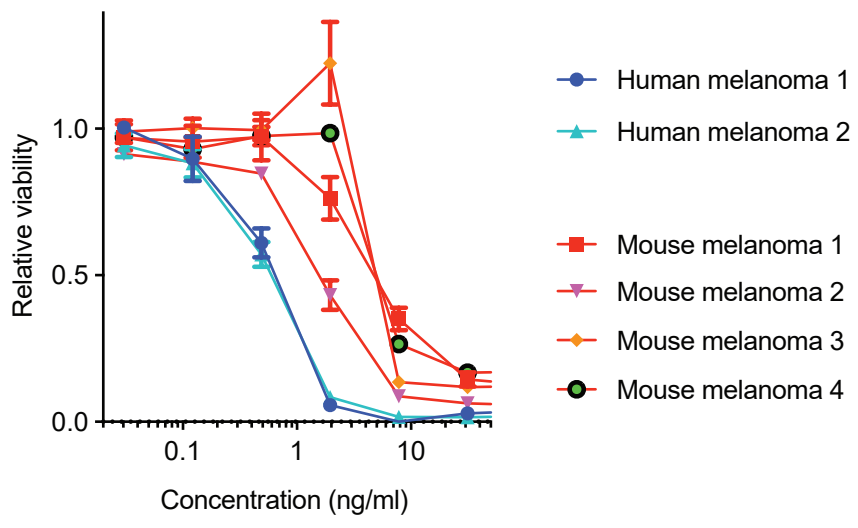
Suppl. Figure 1.



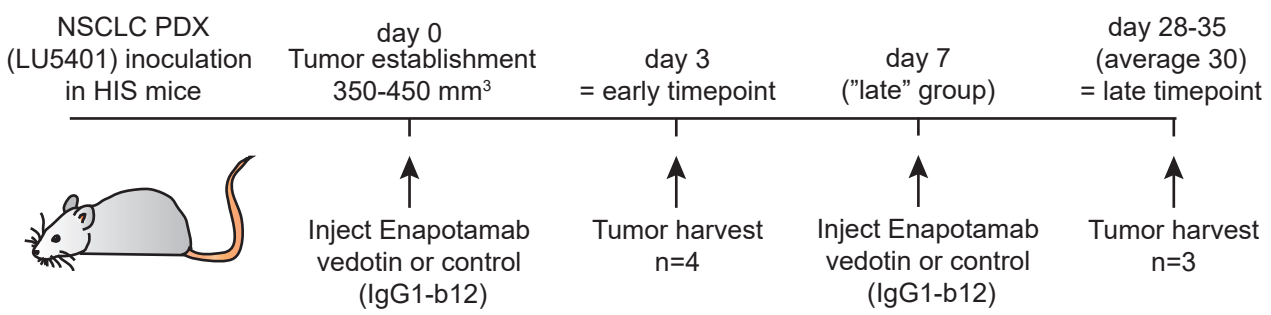
Suppl. Fig. 1. EnaV induces an inflammatory response in PDX models of lung cancer *in vivo*. (A) Growth curves of PDX LXFA526 and 677 *in vivo* and efficacy of EnaV (2 and 4 mg/kg). IgG1-b12-MMAE and IgG1-b12 were used as controls. Error bars represent SEM. Statistical analysis by Mann-Whitney test; ** $p < 0.01$. (B) AXL positivity of the two tumor models of panel A. (C) Graphic overview of experiment performed for RNA + proteomic sequencing. (D, E) Principal component plots of the gene expression data combined for both PDX models, showing treatment-related separation in PC3. (F) Heat map of the EnaV gene expression signature in PDX tumors treated with Ctrl (IgG1-b12) or EnaV (4 mg/kg) for 3 days. (G) Proteomics analysis on day 3 after EnaV/Ctrl treatment of the same tumors used for RNA profiling. Q-value of < 0.1 and fold change of > 1.5 were used as cut-off. Green dot indicates significant hit in the interferon response pathways. (H) qPCR quantification of *IFIT1-3* and *MX1* in three LXFA526 tumors from the *in vivo* experiment as described in panel C. Mice were treated with EnaV or control IgG1-b12 and tumors were harvested after 6 days for RNA isolation.

Suppl. Figure 2.

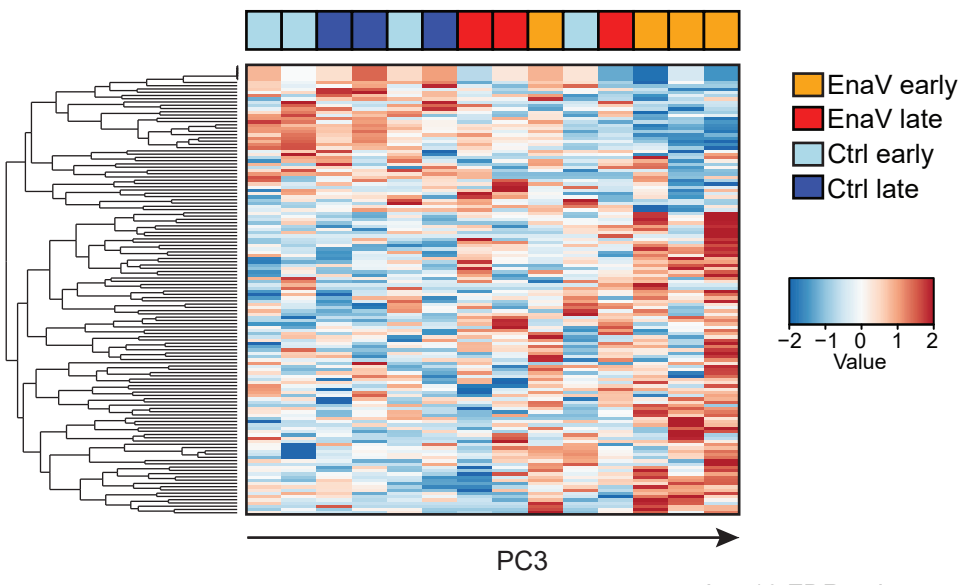
A.



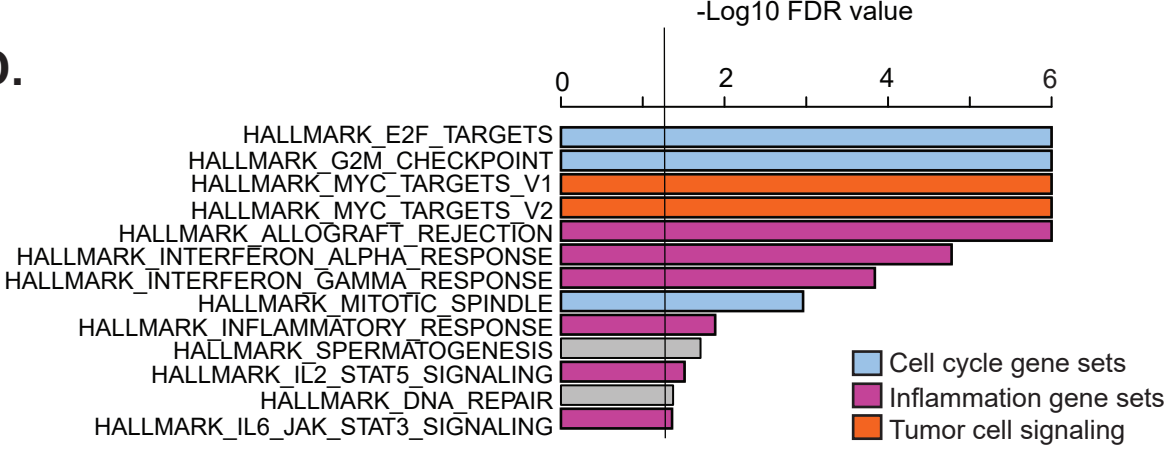
B.



C.

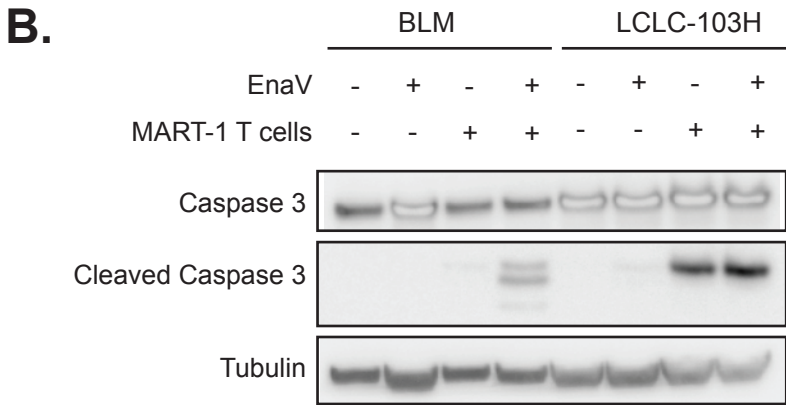
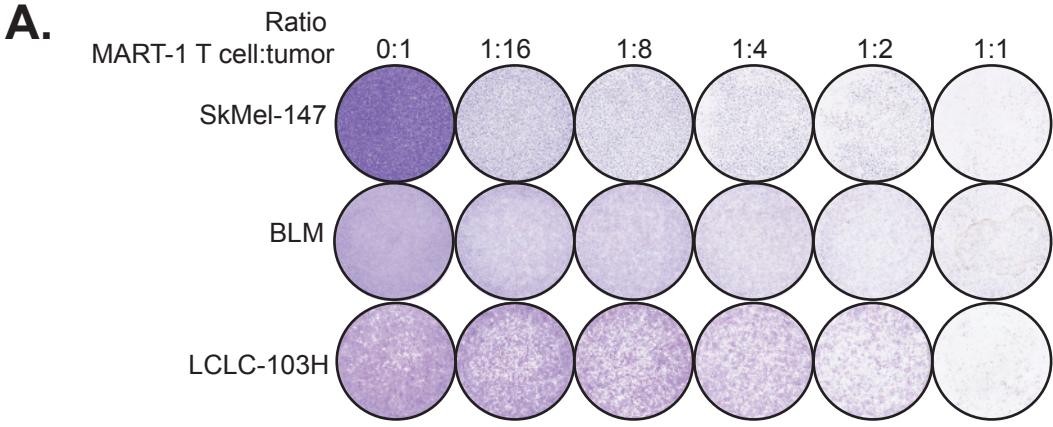


D.



Suppl. Fig. 2. Profiling of lung cancer PDX LU5401 in HIS mice. (A) Sensitivity to free MMAE of human (blue) and mouse (red) cell lines. (B) Graphic overview of experiment performed for RNA sequencing. Tumors were used for the analysis of panels B and C. (C) Heat map of the EnaV signature in LU5401 PDX tumors treated with either Ctrl (IgG1-b12) or EnaV (4 mg/kg) for 3 days or an average of 30 days (range 28-35). (D) GSEA of comparison between Ctrl ADC (IgG1-b12-MMAE) versus EnaV treatment in LU5401 PDX tumors, showing significantly induced inflammation-associated hallmark gene sets.

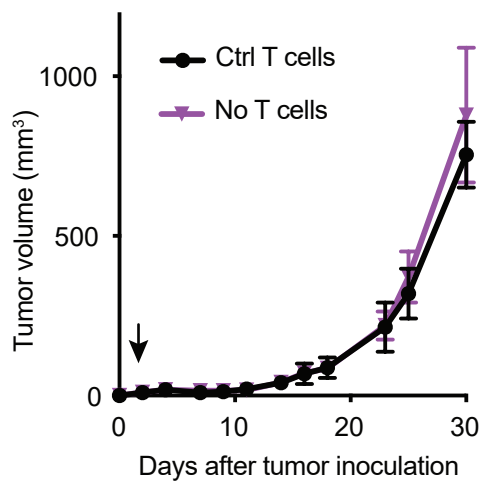
Suppl. Figure 3.



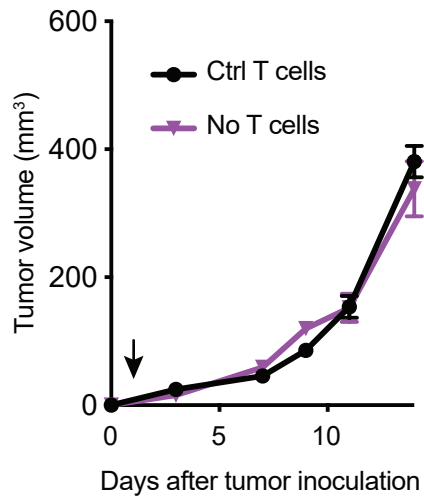
Suppl. Fig. 3. Cell lines treated with EnaV and/or tumor-specific T cells. (A) Colony formation assay of three cell lines, transduced with MART-1+HLA-A2, treated with MART-1 specific T cells for 24 hours in the indicated ratios. Afterwards, T cells were washed away and plates were stained with crystal violet after 3 days. **(B)** Western Blot analysis of cleaved Caspase 3 in melanoma (BLM) and lung cancer (LCLC-103H) cells treated with EnaV (2 µg/ml) or MART-1-specific T cells (in a 1:4 T cell: tumor cell ratio), their respective control treatments (IgG1-b12-MMAE or Ctrl T cells), or the combination for 20 hours. Tubulin was used as a loading control.

Suppl. Figure 4.

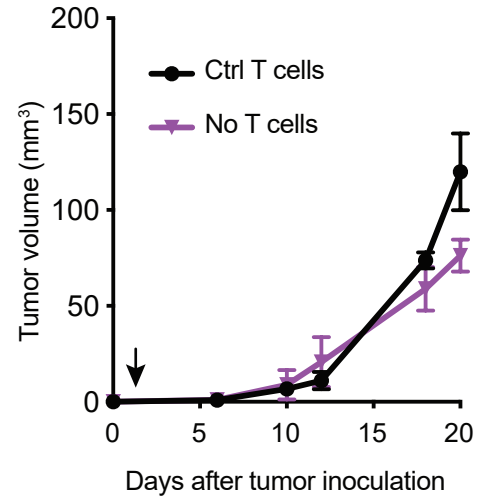
SkMel147



BLM

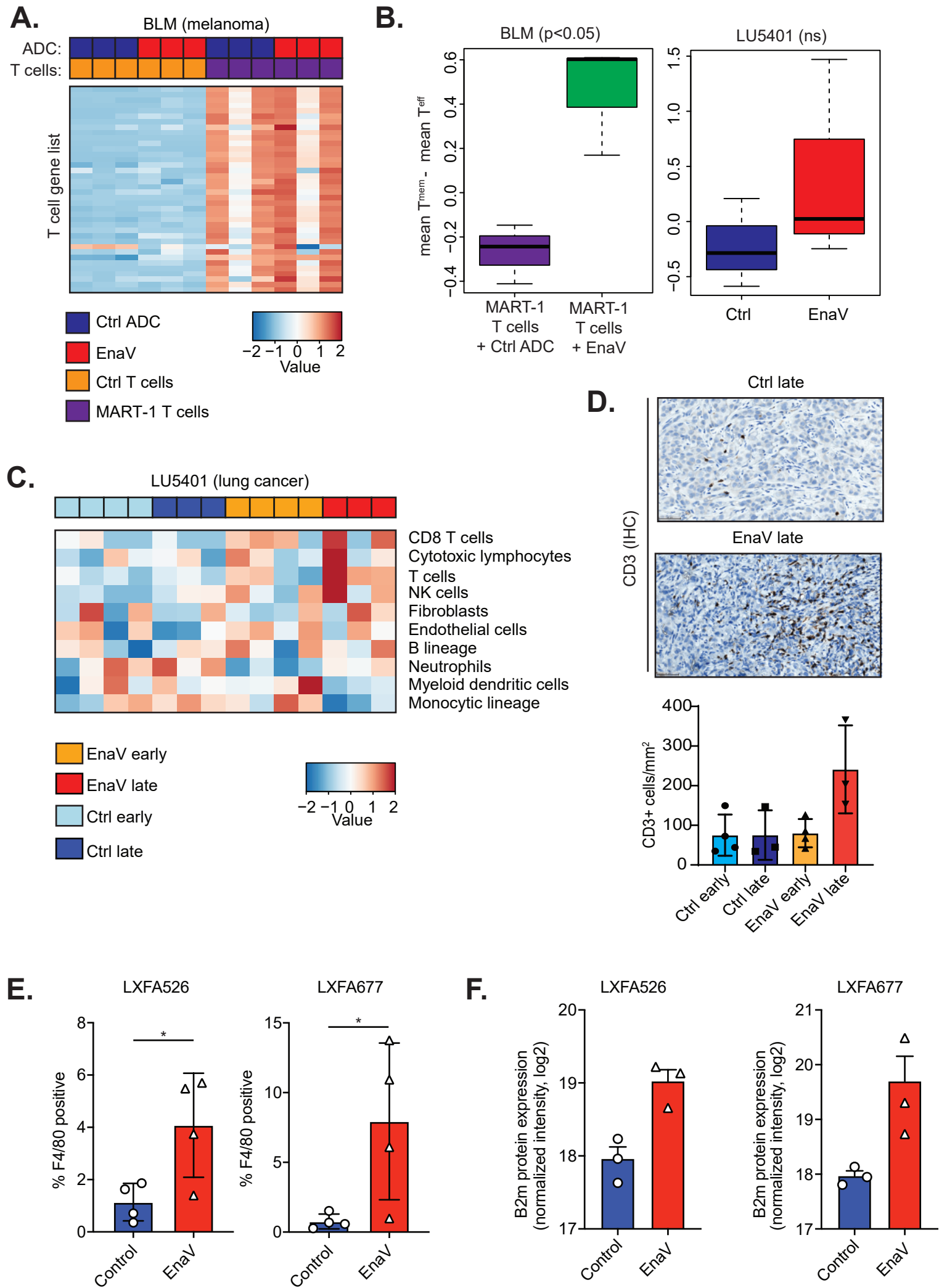


LCLC103H



Suppl. Fig. 4. Sensitivity of melanoma and lung tumors *in vivo* to untransduced versus no T cells.

Suppl. Figure 5.



Suppl. Fig. 5. Immune infiltration in melanoma and lung tumors *in vivo*. **(A)** Heat map of T cell gene sets in EnaV +/- MART-1 T cell treated mice bearing melanoma BLM tumors. **(B)** Mean log value of T memory versus T effector gene set in models from panel A and B. The “late” timepoint of 28-35 days is plotted for LU5401. **(C)** Heat map of immune cell gene sets in EnaV-treated HIS mice bearing LU5401 lung cancer PDX tumors. Immune signature abundance was imputed using MCP counter. **(D)** Representative IHC images of CD3 expressing T cells infiltrating in LU5401 tumors, showing a control tumor at day 30; and an EnaV-treated tumor at day 30. Below: quantification of CD3+ cells per surface area (mm²) in indicated conditions. **(E)** Quantification of F4/80 positive cells by IHC in two lung cancer PDX models, as depicted also in Supplementary Figure 1C. Statistical analysis by unpaired t-test; * p<0.05. **(F)** Quantification of mouse B2m expression by proteomics in two lung cancer PDX models.